Feeling spindle for process force measurement in tool grinding

B. Denkena, H. Klemme, H. Buhl
Institute of Production Engineering and Machine Tools (IFW), Hannover, Germany

Abstract

During tool grinding of workpieces with a large length-to-diameter ratio, process forces cause high deflections impairing the machining accuracy. To reduce such workpiece deflections, a support steady rest is commonly used. However, the support steady rest increases manual set-up effort, thereby decreasing productivity. In order to substitute the support steady rest, an innovative approach is to calculate the workpiece deflection by measuring the process forces using a compliance model. "Feeling" machine tools with structure-integrated force sensing capabilities are a promising approach to detect such process forces. In order to achieve high measurement accuracies when measuring the process forces, structure-integrated sensors must be placed close to the process. Therefore, a novel sensory grinding spindle is being developed for grinding of tools guiding the workpiece during machining. Sensors are integrated into the shaft, thereby enabling process force measurement during the tool grinding process. Equipped with semiconductor strain gauges and a contactless data transmission, the sensory spindle is able to measure the process forces acting on the workpiece and thus to provide force measurement data with high signal quality. With the introduced concept, forces with a resolution of higher than $\sigma = 3.7$ N were measured.

1 Introduction

When grinding long projecting solid carbide tools for milling and drilling, one flute is machined in a single grinding operation. The so-called deep grinding requires a high infeed. Due to the high infeed and high feed rates v_f, high process forces act on the tool blank. The radially acting force F_N leads to a displacement $\Delta w(L)$ of the tool blank depending on the location of the grinding wheel engagement and the area moment of inertia (Fig. 1). This displacement in

turn leads to shape deviations and geometric errors, such as significantly higher core diameters of the workpiece.

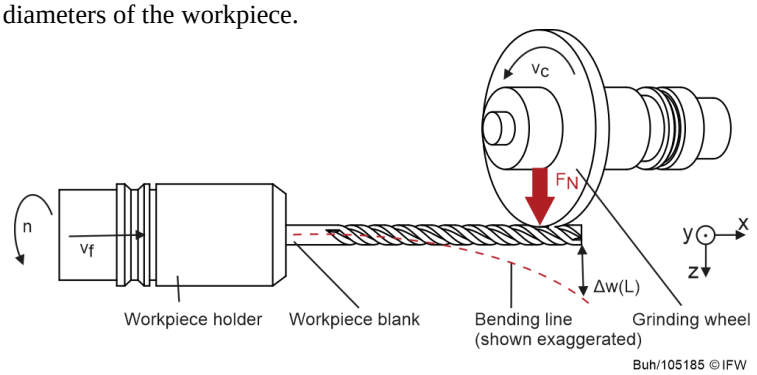

Figure 1: Displacement during tool grinding process

Currently, a steady rest (not shown in Fig. 1) is used to counteract the radially acting force, especially for workpieces with a high length-to-diameter ratio (L/D > 8). However, setting up the steady rest requires significant effort, as the position of the steady rest must be adjusted manually for each workpiece geometry. Alternatively, a reduction in workpiece displacement can be achieved by reducing the feed rate. However, the feed rate must be iteratively adjusted to the respective workpiece geometry, which also reduces productivity. In order to increase the machining accuracy while maintaining high productivity, a new approach of real-time displacement compensation is being researched. Based on a force-sensitive grinding spindle, online measurement of the process forces is being investigated. Furthermore, a simplified compliance model is derived for calculating the resulting displacement Δw(L) using the measured process forces. Subsequently, the calculated displacement is compensated by an adjusted axis infeed of the tool in the NC code during the process.

Today, process forces can be determined during machining with sensory tool holders or with integrated force sensors. However, the significantly higher set-up effort and the high costs of the sensory tool holders are disadvantageous. These disadvantages do not exist with machine-integrated measuring technology. However, in order to achieve high sensitivity and measuring accuracy with machine-integrated measuring technology, the sensors must be located as close as possible to the process. By means of piezo-electric sensors [BYR07] or shear sensors [ALT04] mounted into the force flow between the spindle housing and the spindle flange, it is possible to measure process forces close to the process without influencing the working area. These additional sensors can also be used for condition monitoring and process monitoring during milling and drilling. However, sensors between the spindle housing and the spindle flange reduce the rigidity of the connection between the spindle and the machine structure. This approach is not feasible for a grinding process with high rigidity and accuracy requirements. In [ALT92], an approach is presented with which the process forces can be reconstructed via the signals of the feed drive current without additional sensors. However, only a force resolution of σ = 52 - 75 N is achieved. This is too high for determining the process forces in tool

grinding, as preliminary investigations have shown that a resolution of less than $\sigma = 10$ N is required. In [BOU22], a retrofit concept for a sensor integration into a spindle based on strain gauges is presented, which does not affect the stiffness. However, only a resolution of the radially acting force by $\sigma = 40$ N is achieved. Moreover, this concept cannot be used on spindles without a non-rotating flange, as in tool grinding. However, the research of smart and intelligent spindles is a forward-looking topic, so that smart spindles are also being researched in other areas of application, such as in [WAN17] and [KER08].

Based on the current state of knowledge, there is no concept for measuring the radially acting force close to the work spindle during tool grinding and for achieving a resolution of at least $\sigma = 10$ N. Therefore, in this paper, the design of a sensory grinding spindle based on strain gauges applied to the spindle shaft and a further optimization of the sensitivity of the sensor system by notches are presented in Section 2. Additionally, the characteristics of the prototypical sensory grinding spindle are examined. In order to further increase the sensitivity a sensor fusion is presented in Section 3.

2 Design of the sensory grinding spindle

For the grinding of tools, two spindles are used synchronously. The workpiece spindle guides the workpiece in a rotational-linear motion relative to the tool (grinding wheel). The second spindle drives the tool. As the spindle shaft of the workpiece spindle only rotates at low speeds ($n < 500$ min^{-1}), the centrifugal forces acting on the sensors are correspondingly low and interference effects in the recording of measurement data and in the transmission of the energy and measurement data are potentially negligible. Consequently, this spindle is chosen for the integration of the sensors. However, only limited installation space is available on the spindle shaft for the integration of the sensor system. Furthermore, a wear-free energy and data transmission is required so that no damage to the spindle occurs due to abrasive particles in the bearings.

2.1 Sensor positioning for high sensitivity

External loads cause machine components to deform elastically and strain occurs on the component surfaces. These strains can be measured by strain gauges (SG) and converted into an electrical measured variable. For the concept of the sensory spindle, highly sensitive semiconductor strain gauges (SC-SG) of the type SSGF-060-033-500PB-M4 from Haptica S.r.l. are used as a full bridge with a resistance of 540 Ω. Full bridge SG have the advantage that transverse expansions and thermal influences have a reduced effect on the measurement signals. These SC-SG have already been successfully tested in rigid machine components (e.g. swivel clamps) and have an amplification factor that is about 70 times higher than of metallic foil strain gauges [DEN21].

To identify a suitable position of the SC-SG, the workpiece spindle was analyzed by means of the finite element method (FEM). In addition, the

plausibility of the FEM simulation was checked using a network study. In previous experimental investigations, the expected displacement force during deep grinding of tools was identified with a value of $F_N = 200$ N. This displacement force was applied to the spindle shaft with the help of a remote point. The spindle housing was defined as stiffly fixed to the environment. The bearings were modelled according to the corresponding radial and axial bearing stiffnesses of the manufacturer's specifications. In Fig. 2, the design of the spindle front and the identified areas with high strain are shown.

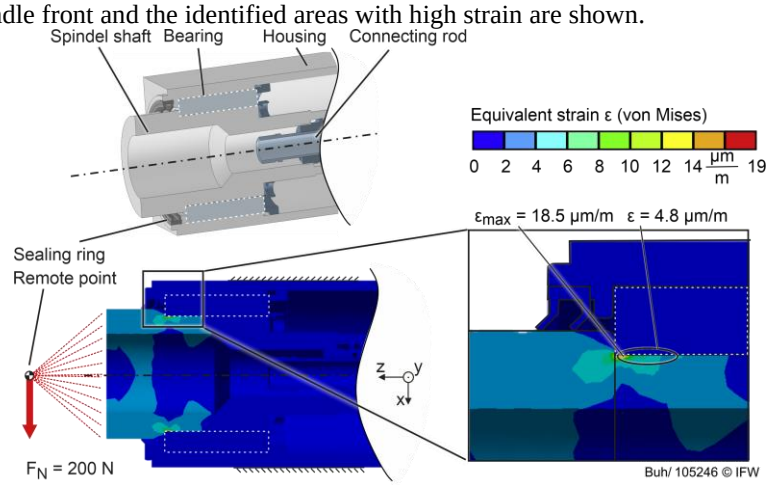

Figure 2: Analysis of the maximum strain for sensor positioning

The results of the FE-simulation show that the simulated mean strain in the area of the bearing seat is $\varepsilon = 4.8$ µm/m. The highest strain ($\varepsilon_{max} = 18.5$ µm/m) is present on the edge of the bearing seat. However, this strain is present in a locally very limited area. High strains lead to a high sensitivity of the SG, but are only suitable if they occur homogeneously over the entire contact area of the SG. Therefore, in the shown case, the strain distribution and the value must be optimized by a geometrical adaption of the bearing seat area to homogenize and, if possible, to increase the strains and thus to achieve a highly sensitive sensory grinding spindle.

2.2 Sensitivity increase through modified notch geometry

It is known that the strain and thus, the sensitivity of SG can be significantly increased by using the notch effect [BOU19]. In addition, a more homogeneous distribution can be achieved. The challenge is to achieve a higher local strain at the same force without significantly weakening the stiffness of the spindle. The notch geometry used in [DEN13] has been designed for use in flat structures. However, it is currently unknown which geometry parameters of a notch are suitable for use in rotationally symmetrical bodies. Therefore, different notch geometries were investigated using FEM. Figure 3 shows the strain distribution of the respective shaft section without a notch (a), the results with a trapezoidal notch geometry from [BOU19] (b), and the notch geometries E (c), F (d) and H

(e) according to DIN 509. The mean strains $\varepsilon_{a\text{-}e}$ occurring in the notches are shown in the figures below. Due to the installation space, the width of the notch is fixed with a value of $\Delta z = 8.0$ mm.

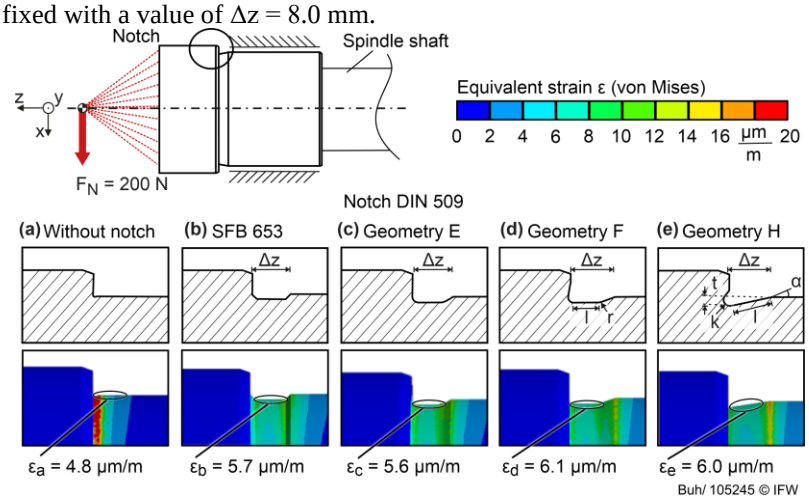

Figure 3: Analysis of the maximum strain for sensor positioning

The results of the investigation show that by introducing the notches (b) to (e), a more uniform strain distribution is achieved on the surface of the shaft surface than without the notch (a). When comparing the notch shapes, F (d) and H (e) have the two highest mean strains. The trapezoidal geometry (b) and the geometry E (c), on the other hand, have the lowest mean strains. However, despite the highest strain, the dimensions of the geometry F (length of flat surface l = 4.9 mm) are too small for the application of the provided SC-SG (length: 7.9 mm; width: 5.2 mm). The SC-SG would have to be applied to the radius beyond the flat area of the notch. However, it is not possible to apply the SC-SG to small radii of $r < 1.5$ mm. Therefore, the geometry H was chosen for the realization of a prototype of the sensory spindle.

In order to further maximize the mean strain, geometry optimization was performed using a design-of-experiment (DoE) [DEN22]. With the DoE, the geometry parameters notch depth t, radius k and angle α were varied in a partial factorial simulation to determine their influence on the achievable mean strain. With the optimized values of the notch parameters, a mean strain of $\varepsilon = 6.7$ µm/m was simulated. The static stiffness of the spindle shaft is reduced by less than 1% with the modified notch. However, by means of the optimized notch geometry, the sensitivity is increased by 37.5% compared to the spindle shaft without a notch.

3 Experimental sensitivity analysis

3.1 Force measurement with the sensory grinding spindle

For the implementation of the sensory grinding spindle according to the previous design, a spindle shaft with the optimized notch geometry was manufactured. In addition, four recesses were made symmetrically on the circumference of the shaft to accommodate the electrical peripherals (evaluation board, battery, transmitter unit, energy management) (Fig. 4a, 4c). Four SC-SG were glued into the notch on the circumference at 90° intervals so that the strains in each cartesian axis direction can be measured by means of two SC-SG. The assembled grinding spindle was then mounted on a test rig (Fig. 2b). By means of a piezo actuator (Piezosystem Jena PSt 1000/16/150/ VS25), static and dynamic forces can be applied radially to the spindle shaft via an adapter. A load cell (ME-Messsyteme KM26z-2kN) is mounted between the piezo actuator and the adapter in order to measure the occurring loads (Fig. 4b). The transmitted measurement data of the SC-SG on the spindle shaft are received by an antenna and recorded by an industrial PC. By means of the same industrial PC, the piezo actuator is controlled to apply a load F to the spindle shaft. With this setup, a data recording of the SC-SG with a frequency of $f_{SG} = 526$ Hz and a data recording of the force sensor with a frequency of $f_F = 1{,}000$ Hz is achieved.

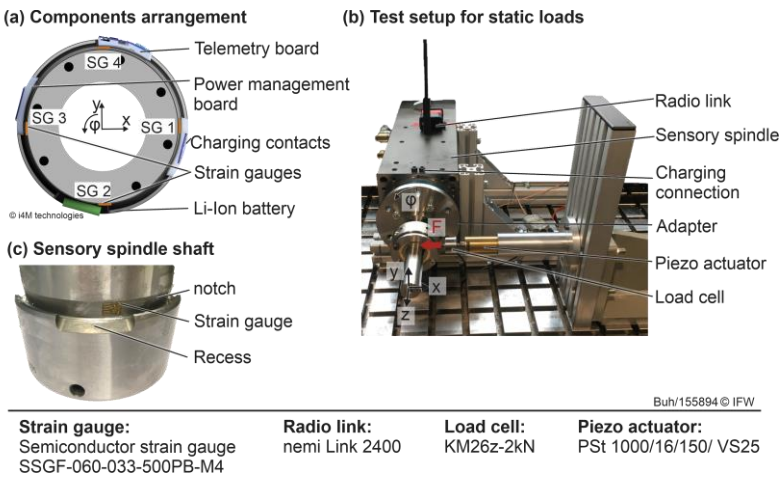

Figure 4: Sensors on the spindle shaft and test setup

In order to investigate the sensitivity of the sensory grinding spindle, load collectives are applied radially to the spindle shaft and the load as well as the measurement signals from the SC-SG are measured continuously. The load is increased stepwise in five steps from F = 0 N to 230 N, whereby the spindle shaft is aligned with a rotation angle of φ = 0° (load in x-direction) and to φ = 90° (load in y-direction). Figure 5 shows an example of the SG-signals U for SG 1 (blue) and SG 2 (green) as well as the applied load F (black) as a function

of time t for the respective load direction. In Fig. 5a, it can be seen for the load in the x-direction that the SG-signals U of both SC-SGs show the defined step-shaped curve of the reference load F. The signal of SG 1, shows a signal 375% higher than that of SG 2. In contrast, SG 2 shows a signal 320% higher than that of SG 1 for loading in the y-direction (Fig. 5b). This is explained by the fact that the SG that are aligned with the load direction provide the larger signals due to the higher strains. The fact that the strain gauges placed orthogonally to the load direction (SG2 in Fig. 5a and SG1 in 5b) show signals higher than 0 mv/V is due to the fact that the angle of rotation was set manually and thus with some positioning errors. The differently distinct courses of the SG-signals SG1 (a) and SG2 (b) related to the load is due to a different sensitivity of the SG. This is examined in more detail in 3.2.

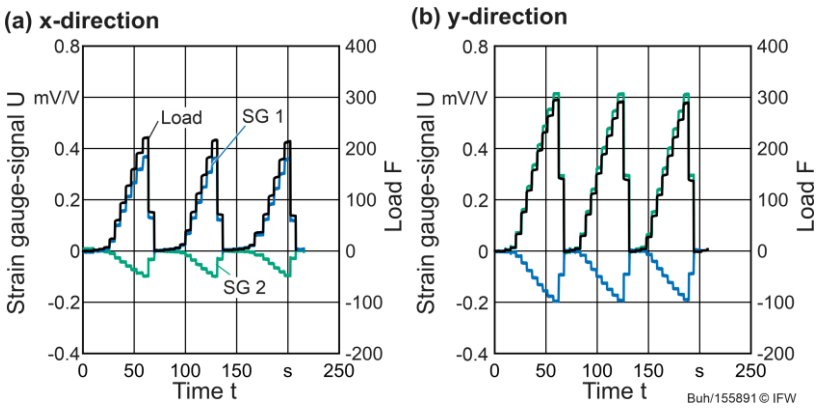

Figure 5: Measurement signals of the sensory spindle under static load

The results of the investigation show that continuous measurement of the load is possible and that there is a proportional correlation between the external load and the measured change in resistance of the SC-SG.

3.2 Directional sensitivity of the sensory grinding spindle

In order to derive the applied loads from the measured SG-signals, a conversion of the SG-signals into force values via a proportionality factor is required. From the previously measured SG-signals and forces (Fig. 5), the load F and the associated SG-signals U can be extracted at the individual load levels. Figure 6 shows the measured SG-signals U as a function of the defined load F in the x-direction (a) and the y-direction (b).

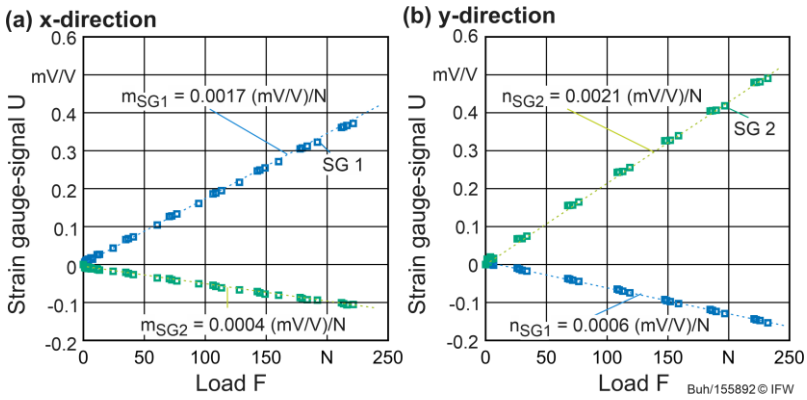

Figure 6: Directional sensitivities of the sensory grinding spindle

The courses of the individual measuring points of the SG-signals exhibit a strictly linear correlation, so that an approximation is made with a first-degree function. The gradient of the linear approximation function corresponds to the sensitivity of the strain gauge with regard to the external load. For SG 1, a load in the x-direction results in a sensitivity of m_{SG1} = 0.0017 (mV/V)/N, while SG 2 has a 77% lower sensitivity of m_{SG2} = 0.0004 (mV/V)/N. In contrast, in the y-direction, SG 1 has a 72% lower sensitivity (n_{SG1} = 0.0006 (mV/V)/N) than SG 2 (n_{SG2} = 0.0021 (mV/V)/N). The fact that the amplitude of the signal of SG 2 is lower than of SG 1 when loaded in the x-direction is due to the fact that only small shear strains occur in the bending axis. This shear strains are measured by the full bridge strain gauge but do not have an impact on the measurement of any other sensor because each signal is processed individually. Furthermore, a measured strain of ε_m = 4.3 µm/m can be inferred from the strain gauges measurement data. This corresponds to 64.2% of the expected strain from the FEM. The deviations between the measured and the simulated strains can be attributed to the glued connection, the manual sensor positioning and the force application on the test rig.

The approximation of the courses of the measured data with a first-degree function shows a high regression quality with a coefficient of determination of R^2 = 0.97. Due to the fact that the sensitivities m_{SG1} and n_{SG2} of the individual SG 1 and SG 2 differ by 23.5%, a direct calculation of the measured signals of only one SG for the reconstruction of the load is not possible. In order to reduce the influence of disturbance variables, the coupling effects and to determine the sensitivity independently of the direction, a sensor fusion is suitable.

3.3 Sensitivity enhancement via sensor fusion

To further increase the sensitivity to external loads by means of the SG-signals and reduce the influence of the coupling effect, a sensor fusion of the four SG-signals is performed. By means of a weighted calculation of all SG-signals in a sensor fusion (Eq. 2 and Eq. 3) with the weighting factors a to h, the sensitivity per load direction can be increased. In addition, the aim is to

determine the sensitivity of the SG-signals independently of the angle of rotation of the spindle shaft. Aligning the sensitivities of the fused SG-signals in the x-direction (SG_x) and y-direction (SG_y) has the advantage that a force reconstruction of a resulting radial force along the entire angle of rotation (φ = 0° - 360°) is possible by means of a direction-independent sensitivity.

$$SG_x = (a \cdot SG\,1 - b \cdot SG\,3) - (c \cdot SG\,2 + d \cdot SG\,4) \quad \text{(Eq. 2)}$$
$$SG_y = (e \cdot SG\,2 - f \cdot SG\,4) - (g \cdot SG\,1 + h \cdot SG\,3) \quad \text{(Eq. 3)}$$

The fused signals SG_X and SG_Y are shown in Fig. 7a exemplarily for a load in x-direction. The basis for this evaluation is the measurement data from Fig. 5. For the fused SG-signal SG_x (blue), the sensitivity factor is $m_{SG,x}$ = 0.0026 (mV/V)/N, resulting in a 53% increase in sensitivity compared to the single SG-signal of SG 1. For the fused SG-signal SG_y (yellow), a sensitivity factor of $m_{SG,y}$ = 0.0025 (mV/V)/N is determined. This also results in a 19% increase in sensitivity in the y-direction compared to the single SG 2. The two fused sensitivities deviate from each other by 3.9%, so that the deviations are minimal and a direction-independent sensitivity can be assumed. Fig. 7b shows the curves of the fused SG-signals and the force curve of the identical measurement from Fig. 5a. The increase in sensitivity results in a higher amplitude of the measurement signal for the fused measurement SG_x under load in the x-direction. In addition, the fusion reduces the interference for the measurement signal in the y-direction. This can be seen from the low amplitudes of the measurement signal of the fused SG_y (Fig. 7b) compared to the measurement signal SG 2 (Fig. 5a). With sensor fusion, a minimal force reconstruction resolution of σ = 3.7 N is achieved. This corresponds to the minimum force that can be unambiguously detected without the noise of the two signal plateaus overlapping.

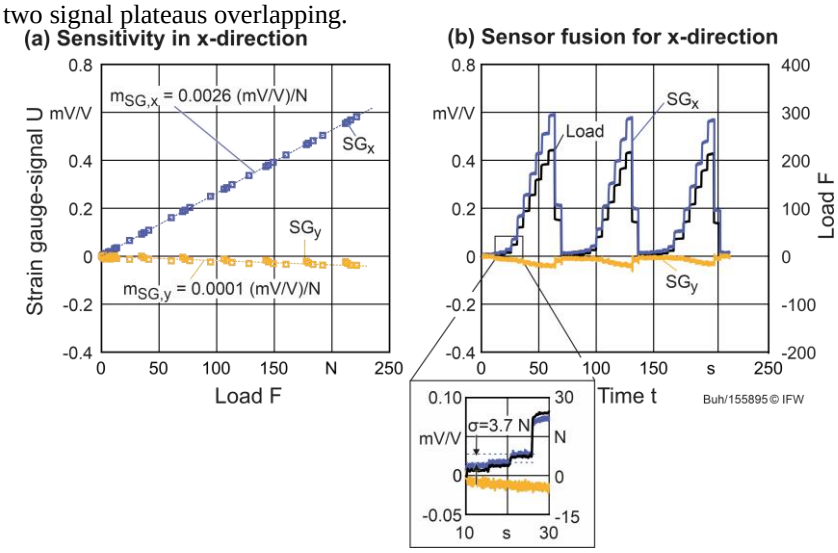

Figure 7: Sensitivity increase through sensor fusion

The sensor fusion results indicate that by offsetting multiple strain gauge signals, a significantly higher sensitivity is obtained. In addition, the directional dependence of the sensitivity is extracted so that a uniform sensitivity can be used for later force reconstruction.

4 Conclusion & Outlook

In this paper, the design of a sensory grinding spindle, as well as the metrological investigation for force reconstruction based on structure-integrated semiconductor strain gauges are presented. First, sensor positions were identified by means of finite element simulation and a notch geometry was optimized in order to obtain the highest possible and homogeneously distributed strain at the sensor position. Subsequently, a prototype of the sensory grinding spindle was built and characterized in terms of functionality and sensitivity. A linear correlation between the strain and the strain gauge signal was identified and the sensitivity was determined as a proportionality factor. In addition, it was presented that, by means of sensor fusion, the sensitivity could be further increased up to $m_{SG} = 0.0025$ (mV/V)/N. The developed sensory grinding spindle allows the measurement of an external radial load on the spindle shaft with a minimal resolution of $\sigma = 3.7$ N. In the future, the sensory grinding spindle will be integrated into a machine tool and a calibration will be done to calculate the radial process forces. The sensory spindle enables online force measurement during grinding and thus online displacement compensation during tool grinding.

Acknowledgements

The results presented were obtained within research project “Productivity increase in tool grinding with the help of a “feeling” spindle” (417859800)”. The authors thank the German Research Foundation (DFG), the “Sieglinde Vollmer Stiftung” and the VOLLMER WERKE Maschinenfabrik GmbH for their support.

References

[1] Altintas, Y.: Prediction of Cutting Forces and Tool Breakage in Milling from Feed Drive Current Measurements, Journal of Engineering for Industry ASME, Vol. 114, p. 386-392, 1992.

[2] Altintas, Y.; Park, S.S.: Dynamic Compensation of Spindle-Integrated Force Sensors, CIRP Annals, Vol.53/1, p.305-308, 2004

[3] Boujnah, H.: Kraftsensitiver Spindelschlitten zur online Detektion und Kompensation der Werkzeugabdrängung in der Fräsbearbeitung, Dr.-Ing. PhD, Gottfried Wilhelm Leibniz Universität Hannover, 2019.

[4] Boujnah, H.; Irino, N.; Imabeppu, Y.; Kawai, K.; Mori, M.: Spindle-integrated, sensor-based measurement system for cutting forces, CIRP Annals – Manufacturing Technology, 71, p. 337-340, 2022.

[5] Byrne, G.; O'Donnell, G.E.: AN Integrated Force Sensor Solution for process Monitoring of Drilling Operations, CIRP Annals, Vol. 56/1, p. 89-92, 2007.

[6] Denkena, B.; Litwinski, K.M.; Brouwer, D.; Boujnah, H.: Design and Analysis of a Prototypical Sensory z-slide for Machine Tools, Production Engineering – Research and Development, 7/1, p. 9–14, 2013.

[7] Denkena, B.; Bergmann, B.; Teige, C.: Die Zukunft der Spanntechnik gestalten - Das IFW Hannover entwickelt im Projekt „TensorMill" ein cyberphysisches Spannsystem, mav, 6, p. 42-45, 2021.

[8] Denkena, B.; Klemme, H.; Buhl, H.: Sensory Grinding Spindle Senses Process Forces During Tool Grinding, ZWF, Vol.117/10, 2022.

[9] Kern, S.; Schiffler, A.; Nordmann, R.; Abele, E.: Modelling and active damping of a motor spindle with speed-dependent dyn-amics, 9th International Conference on Vibrations in Rotating Machinery, pp. 465–475, 2008.

[10] Wang, C.; Cheng, K.;Rabowski, R.; Soulard, J.: An experimental investigation on ultra-precision instrumented smart aerostatic bearing spindle applied to high speed micro-drilling, Journal of Manufacturing Processes, Vol. 31, pp.324-335, 2018.